University of Tartu

Faculty of Science and Technology

Institute of Physics

Physics department

Dmitri Lanevski

POLYCYCLIC AROMATIC HYDROCARBONS DETECTION AT THE SECOND HARMONIC OF EXCITATION WAVELENGTH MODULATION FREQUENCY

Master degree thesis (30 EAP)

Supervisors: Cnd. of P.M.s Koit Mauring

PhD Eric Tkaczyk

Approved for defence .....

~~Juhendaja~~ Programm manager__–.....

signature, date

Tartu 2016

TARTU ÜLIKOOL

Contents

1. Information sheet

A. In English

INTERFERENCE FILTER TILTING FOR DETECTION OF POLYCYCLIC AROMATIC HYDROCARBONS AT THE SECOND HARMONIC OF EXCITATION WAVELENGTH MODULATION FREQUENCY

This thesis presents a practical implementation of the wavelength-modulation spectroscopy technique with second-harmonic detection (WMS-2f) for selective detection and concentration measurements of polycyclic aromatic hydrocarbons (PAHs) - common fossil fuel pollutants. The method is based on excitation light wavelength modulation around the maximum of a narrow peak in the absorption spectrum of a PAH and lock-in detection of fluorescence at the second harmonic of the excitation wavelength modulation frequency. A UV-LED is used as the excitation source and wavelength modulation is performed via narrow-band interference filter tilting. Model computations are presented to estimate the influence of background signal on the sensitivity of the method. Feasibility is demonstrated by presenting a prototype of PAH sensor, which was tested on a carcinogenic PAH, benzo(k)fluoranthene. We were able to detected benzo(k)fluoranthene to a concentration limit of $0.5 \cdot 10^{-9}\ M$.

B. In Estonian

POLÜTSÜKLILISTE AROMAATSETE SÜSIVESINIKE TUVASTAMINE ERGASTUSE LAINEPIKKUSE MODULATSIOONISAGEDUSE TEISEL HARMOONIKUL

Käesolev lõputöö kirjeldab polütsükliste aromaatsete süsivesinikke (PAS) detekteerimise meetodit, mille aluseks on ergastava valguse lainepikkuse modulatsioon ja fluorestsentsi intensiivsuse mõõtmine modulatsioonisageduse teisel harmoonikul. Ergastusvalguse modulatsioon toimub uuritava PAS-i suhteliselt kitsa neeldumismaksimumi ümber. Fluorestsentsi mõõtmine toimub *lock-in* võimendi abil ergastava valguse lainepikkuse modulatsiooni teisel harmoonikul või Fourier sagedusspektri uurimise kaudu. Ergastusvalguse allikaks on UV-LED ja ergastuse lainepikkuse modulatsioon toimub kitsaribalise interferentsfiltri perioodilise kallutamise teel. Töös on toodud meetodi teooria ja sellel põhineva PAS-de detektori prototüübi väljatöötamine. Töö käigus konstrueeritud prototüübi abil on demonstreeritud antud meetodi tundlikkust, selektiivsust ja efektiivsust. Katsed on tehtud kantserogeense PAS-ga – benso(k)fluoranteeniga. Piirtundlikkuseks on saavutatud 0.5 ppb.

CERCS codes: P140, P160, P170, P190, P200, P230, P260, P300, P305, P400

2. Introduction

For several decades, it has been generally accepted that polycyclic aromatic hydrocarbons (PAHs) have mutagenic and carcinogenic effects [1]. They have received considerable attention and presently different restrictions and contamination standards imposed on PAH contamination in food [2], consumer products [3], water [4] and air [5] have been established. However, due to forest fires, combustion of fossil fuels and wide usage of other fossil products that are the main sources of PAHs [6], PAH pollution is constantly increasing and negatively affects our environment and health [7–9]. Therefore, there is a great need for accurate PAH detection and concentration measurements.

Traditionally, chromatography and mass-spectrometry [10, 11] techniques are used for PAH contamination analysis and concentration determination, which provide results of high precision and sensitivity but require complex instruments, an expensive laboratory environment, and long processing times. Therefore, these techniques are not suited for real-time measurements that are necessary for effective PAH contamination monitoring and fast pollution-prevention actions. In the present work, we propose an in-solution (methanol, water) PAH detection method based on wavelength modulation spectroscopy (WMS) techniques.

The method utilizes narrow absorption peaks of PAHs and their natural fluorescence. We excite analyte around certain PAH absorption peaks and measure fluorescence with a photodiode. The excitation light wavelength is modulated around a PAH absorption peak at certain frequency. The photodiode signal is fed to lock-in amplifier in order to extract fluorescence signal at 2nd harmonic of excitation light wavelength modulation frequency, which is high in case of PAH presence or low otherwise. This allows to detect PAHs and estimate their concentrations.

Excitation light wavelength modulation coupling with lock-in amplifier detection removes most of the background and noise signal using electronic bandpass frequency filters. As a result, it is possible to detect even weak signals that normally are indistinguishable from noise. This greatly improves sensitivity of absorption measurements, allowing detection of smaller concentrations of studied substances.

Another advantage of WMS methods is their implementation simplicity. One must simply pass wavelength-modulated light through the sample and measure the signal at the frequency of interest. Coupled with fast electronics, online measurements are possible. Therefore, WMAS techniques are greatly suited for real-time PAH detection as demonstrated herein.

3. Wavelength modulation for selective and sensitive PAH detection

The implementation of the WMS techniques for detection of PAHs in solution is possible mostly due to relatively narrow absorption peaks. The absorption peaks of typical PAH in methanol – Benzo(k)fluoranthene – are shown in Fig.1. They can be approximated by local Gaussian:

$$Abs(\lambda) = A_{abs} e^{-\frac{(\lambda-\lambda_0)^2}{2c^2}} \quad (1)$$

A_{abs} is absorption maximum value, λ_0 is the central wavelength of absorption maximum and c is a constant related to the FWHM of peak as $FWHM = 2\sqrt{2ln(2)}c$.

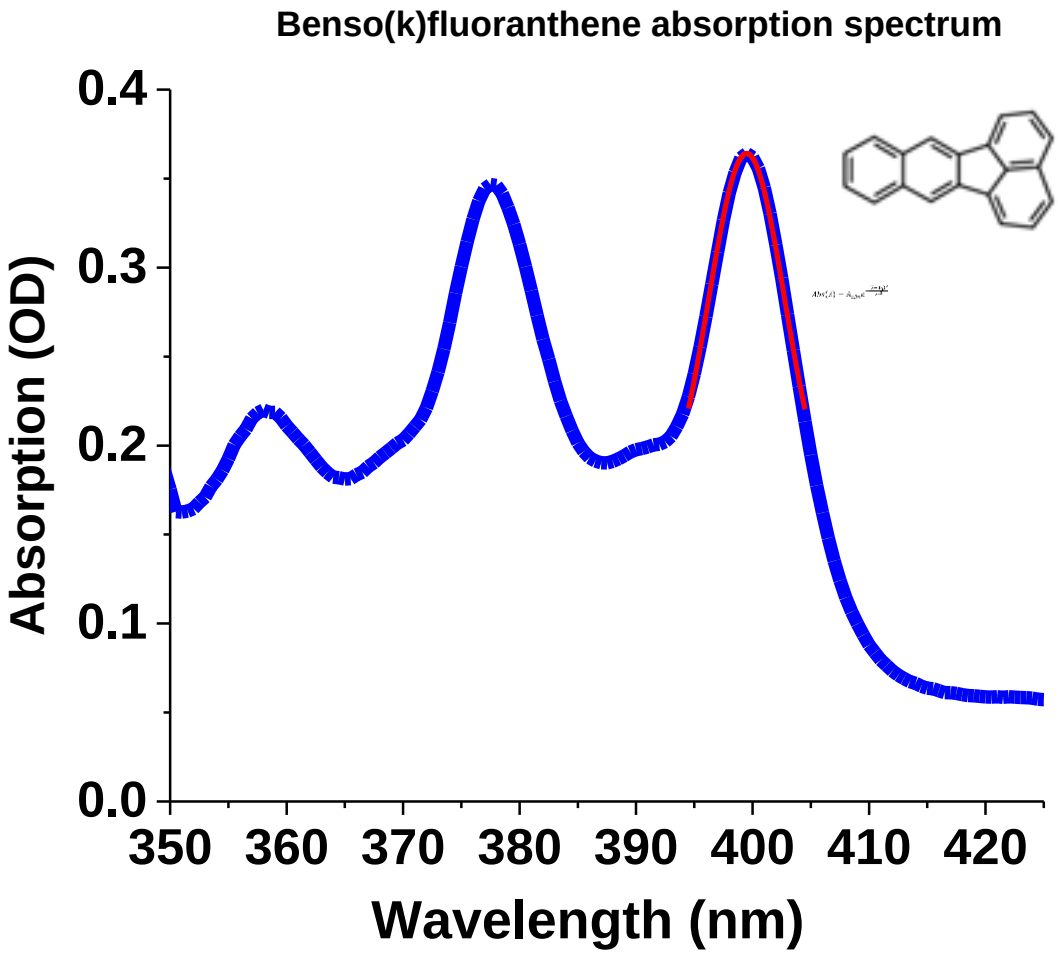

Fig. 1. Drawing showing part of the benzo(k)fluoranthene absorption spectrum (blue line) and a local Gaussian approximation curve (red line) around absorption maximum of 399.5 nm.

The excitation light wavelength modulation can be described by Fourier series:

$$\lambda(t) = \sum_{n=-N}^{N} \Delta\lambda_n e^{i2n\pi ft} \quad \textbf{(2)}$$

Where t is time, $\Delta\lambda_n$is the amplitude of n-th Fourier component, N is number of modulation components and f is a frequency of a modulation. The simplest case of Fourier series, which we also used in our experiments, is a pure sinus:

$$\lambda(t) = \lambda_0 + \Delta\lambda sin(2\pi ft) = \lambda_0 + \Delta\lambda sin(\omega t) \quad \textbf{(3)}$$

This means that in case of wavelength modulation absorption of PAH can be described as

$$Abs(\lambda) = A_{abs} e^{-\frac{(\Delta\lambda sin(\omega t))^2}{2c^2}} \quad \textbf{(4)}$$

The fluorescence intensity dependence from the absorption is described by following equation:

$$I_{fl} = \varphi_0(I_0 - I_T) = \varphi_0 I_0(1 - e^{-Abs}) \quad \textbf{(5)}$$

where I_{fl} is fluoresce intensity, I_0 is incident light intensity, I_T is transmitted light and φ_0 is quantum efficiency.

In practice PAH doesn't dissolve very well in water or methanol and it results in very small optical densities. In this case equation 5 can be simplified and rewritten:

$$I_{fl} = \varphi_0 I_0 Abs. \quad \textbf{(6)}$$

In case of wavelength modulation around absorption maximum is:

$$I_{fl}(t) = \varphi_0 I_0 A_{abs} e^{-\frac{(\Delta\lambda sin(\omega t))^2}{2c^2}} \quad \textbf{(7)}$$

If we assume that wavelength modulation frequency f is 1 Hz ($\omega = 2\pi f$) and make a numerical Fast Fourier Transform of this function (Fig. 2.A), we notice that resulting power spectrum has only even Fourier components with the most significant component at second harmonic of wavelength modulation frequency (means $f = 2\ Hz$).

The other case is the absence of the absorption peak. The simplest model is linear absorption:

$$Abs(\lambda) = Abs_0 + C_{abs}\lambda \quad \textbf{(8)}$$

Where Abs_0 is certain absorption level and C_{abs} is constant defining a slope of linear absorption.

The fluorescence intensity in case of small optical densities and excitation light wavelength modulation can be written as

$$I_{fl}(t) = \varphi_0 I_0\big(Abs_0 + C_{abs}\lambda_0 + C_{abs}\Delta\lambda sin(\omega t)\big) \quad \textbf{(9)}$$

The resulting power spectrum (Fig. 2.B) of the Fourier analysis of this function contains only one component, which is the first harmonic of the excitation light wavelength modulation frequency

(f =1Hz). This means that if we measure fluorescence intensity at the second harmonic (for example by lock-in amplifier), we will get significant signal only if the absorption maximum is present within excitation light wavelength modulation amplitude $\Delta\lambda$. Otherwise the second harmonic signal will be very small or zero as in case of linear absorption, what is a realistic model for absorption background in case of small $\Delta\lambda$.

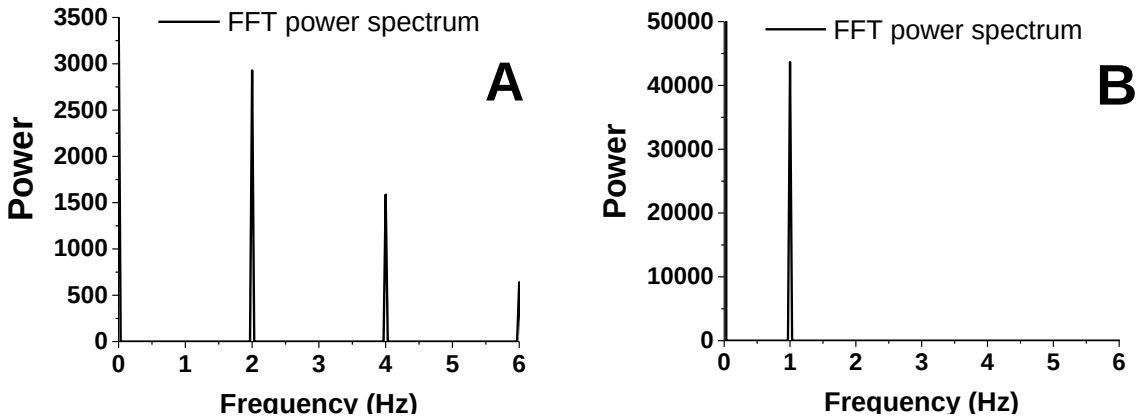

Fig. 2. Power spectra obtained during Fourier analysis of excitation light wavelength modulation around in case of absorption maximum (A) and in case of linear absorption background (B).

Those facts lay the background for the selective detection of polycyclic aromatic hydrocarbons. For example, to detect a benzo(k)fluoranthene, we define an excitation light wavelength modulation amplitude $\Delta\lambda$ symmetrically about one of the absorption peaks of interest. Then we sinusoidally modulate excitation light wavelength with frequency ω in the selected interval $\Delta\lambda$ and measure fluorescence intensity at the second harmonic frequency (2ω). The strong signal is present whenever an absorption peak is present in selected interval $\Delta\lambda$ (Fig. 3).

We could also measure the absorption, but detecting the fluorescence signal provides intrinsically higher SNR than absorption measurements. In particular, fluorescence background depends only on the part of background absorption that also results in fluorescence. If other substances in the analyte fluoresce into the detector, the second harmonic signal 2ω, will be negligible as long as their absorption features are broad enough to change linearly in the wavelength modulation range $\Delta\lambda$.

Quantitative information about PAH can be obtained using Beer-Lambert law for homogeneous solutions in form of

$$Abs = \varepsilon(\lambda)cl \qquad \textbf{(10)}$$

where $\varepsilon(\lambda)$ is extinction coefficient that depends on excitation light wavelength, l is the excitation light optical path length within the sample and c is the concentration of PAH. Substituting this relation into (6) we obtain equation

$$I_{fl} = \varphi_0 I_0 \varepsilon(\lambda) c l \qquad \textbf{(11)}$$

which shows the fluorescence signal dependence on concentration of absorbing particles. We can use this direct proportionality to conduct a quantitative analysis on PAH contamination.

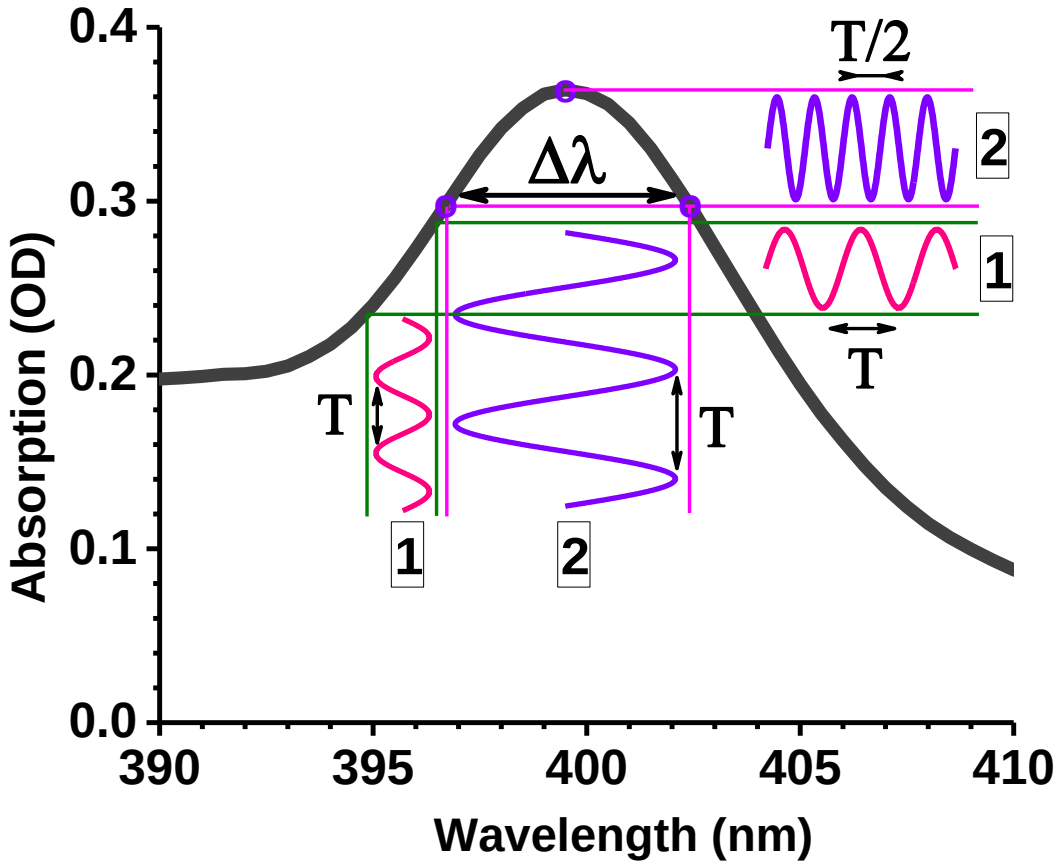

Fig. 3. Drawing showing part of the benzo(k)fluoranthene absorption spectrum and two possible cases that can occur during PAH detection. Nr 2. describes the case when the wavelength modulation is performed symmetrically about the absorption maximum. Nr 1. corresponds to the case when maxima are not present in the selected wavelength modulation range $\Delta\lambda$. Here, sinusoids under the absorption peak depict sinusoidal excitation light wavelength modulation with period T. Sinusoids in the right upper corner show fluorescence intensity waveforms in case of presence (2) or absence (1) of absorption maximum.

4. Mathematical generalization of introduced method

The described above wavelength modulation principle can also be generalized. Consider the fluorescence intensity signal $I_{fl}(t)$ that in wavelength modulation spectroscopy is the overlap integral over λ in each time instant of absorption $Abs(\lambda)$ and excitation spectra $E(\lambda, t)$.

$$I_{fl}(t) = \int d\lambda \, Abs(\lambda) E(\lambda, t) \quad \textbf{(12)}$$

Now let us expand the absorption spectrum about the absorption peak λ_0 as a Taylor series with constants A_n (calculated in usual way from derivatives):

$$Abs(\lambda) = \sum_n A_n (\lambda - \lambda_0)^n \quad \textbf{(13)}$$

And the excitation light spectrum with periodicity ω_0 as a Fourier series with coefficient function $E_m(\lambda)$ (calculated in the usual way from one period):

$$E(\lambda, t) = \sum_m E_m(\lambda) e^{im\omega_0 t} \quad \textbf{(14)}$$

Accordingly, let us decompose $I_{fl}(t)$ into the same Fourier components in terms of harmonics of ω_0:

$$I_{fl}(t) = \sum_m I_m(\lambda) e^{im\omega_0 t} \quad \textbf{(15)}$$

where we calculate using the above 3 equations that I_m is simply the mathematical correlation (at λ_0) of two functions λ^n and E_m:

$$I_m = \sum_n A_n \int d\lambda \, (\lambda - \lambda_0)^n E_m(\lambda) \quad \textbf{(16)}$$

Therefore, in the case that the excitation spectrum is symmetric about λ_0, by cancellation of the integral's negative and positive halves, it becomes clear that for each even m (in particular $m = 2$, the second harmonic), there is no contribution from any odd n (in particular for $n = 1$ in the case of linear component of absorption spectrum). In the case of broken symmetry (as for example if $E(\lambda, t)$ is detuned from λ_0), this may not in general hold.

5. Interference filter tilting as the mechanism for wavelength modulation

C. Sinusoidal wavelength modulation achieved by correct incidence angle calculations

Currently there are existing many different wavelength modulation methods. For example, oscillation of a slit, mirror, diffraction gratings or prism of a monochromator [12]. In present work we decided to use interference filter tilting.

The interference filter transmission central wavelength λ_c is known to depend on angle of incidence θ by a nonlinear equation:

$$\lambda_c(\theta) = \lambda_0\sqrt{1 - \frac{sin^2\theta}{K^2}} \quad \textbf{(17)}$$

where λ_0 is a central wavelength at normal incidence and K is the effective refraction index of the interference filter. However, wavelength modulation with only one Fourier component (i.e. a pure sinusoid) is necessary to avoid second harmonic signals of background fluorescence. The corresponding wavelength modulation waveform is:

$$\lambda(t) = \frac{\lambda_{max} - \lambda_{min}}{2} \cdot \cos(\omega t) + \frac{\lambda_{max} + \lambda_{min}}{2} \quad \textbf{(18)}$$

where λ_{min} and λ_{max} are the limits of wavelength modulation and ω is modulation radian frequency. The appropriate angle time dependence for the filter tilting is therefore:

$$\theta(t) = \operatorname{asin}\left[K\sqrt{1 - \left(\frac{\frac{\lambda_{max}-\lambda_{min}}{2}\cdot\cos(\omega t) + \frac{\lambda_{max}+\lambda_{min}}{2}}{\lambda_0}\right)^2}\right] \quad \textbf{(19)}$$

It was used to calculate the control voltage waveform for the rotating mechanism which had the linear voltage-angle dependence $U(\theta)$. In order to obtain a clean second harmonic signal, the modulation amplitude $\Delta\lambda$ ($\lambda_{max} - \lambda_{min}$, see theory equation 12) was selected as broad as possible and was practically limited by the filter transmission bandwidth (3nm at FWHM) and range of PAH absorption band symmetry about λ_0. For our BKF sample, the following appropriate wavelength modulation parameters were chosen: $\lambda_0 = 404.6\ nm$, $\lambda_{min} = 396\ nm$, $\lambda_{max} = 403\ nm$ and $K = 2.223$. The corresponding excitation light angles of incidence extremums were $\theta_{min} = 11.5°$ to $\theta_{max} = 27.3°$. Wavelength modulation sinusoidality was checked with FSD-9 mini spectrometer by recording interference filter transmission spectra at 10s time interval during 1.75 periods (T=6min) of interference filter tilting. The result, depicted in Fig. 4, confirms high accuracy sinusoidal modulation of wavelength.

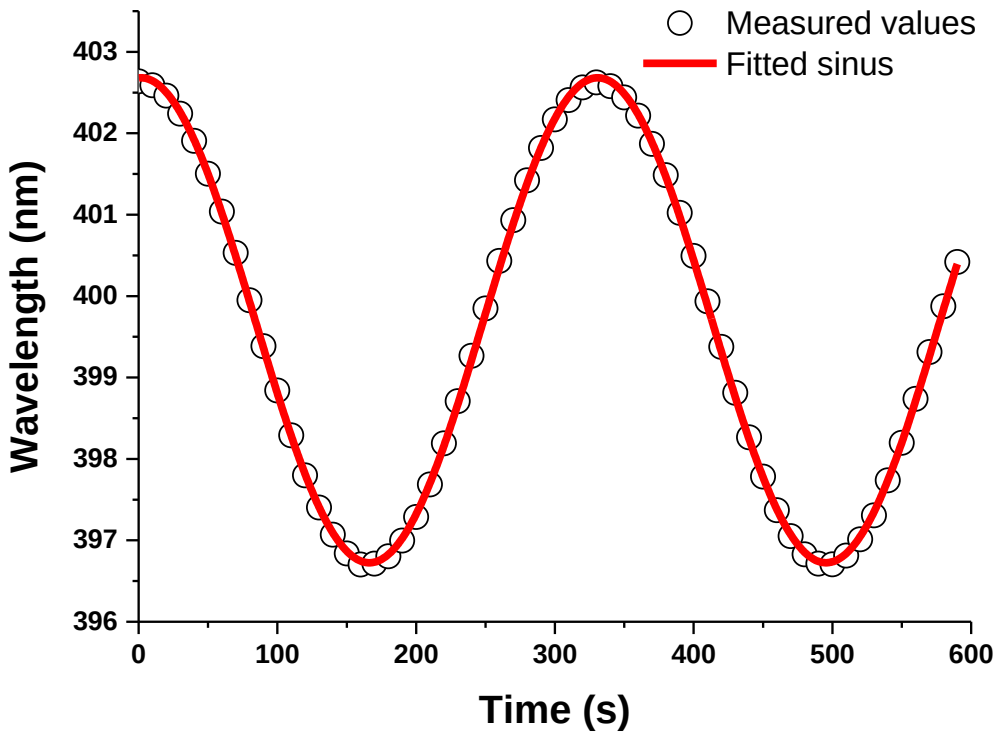

Fig. 4. Excitation light wavelength modulation waveform measured (dots) and approximated with sinusoid (line).

D. Interference filter as a source of unfavorable second harmonic signal

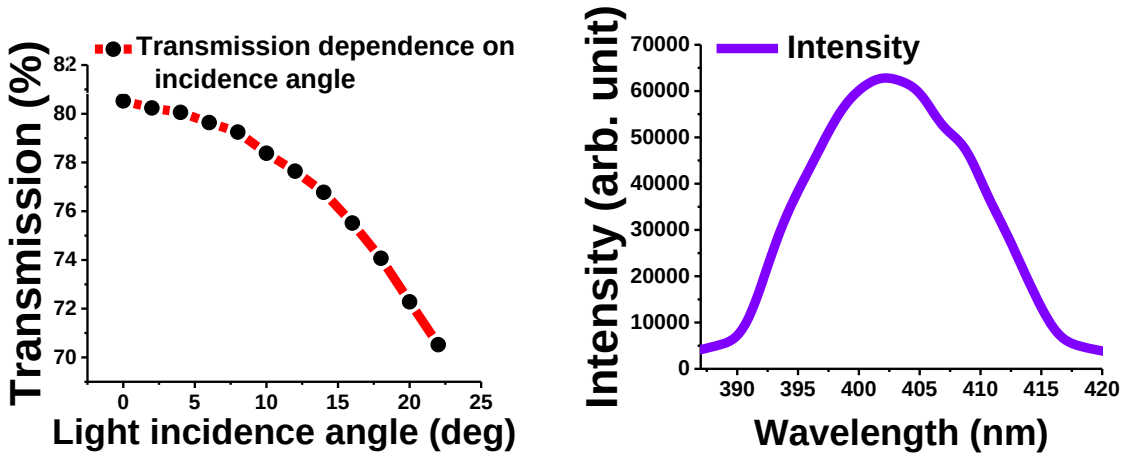

Fig. 5. Experimentally measured interference filter transmission dependence on angle (A) and excitation light source (UV LED LED Bivar UV5TZ-400-30) spectrum (B).

Although interference filter tilting allows to achieve an accurate sinusoidal wavelength modulation, there is other factors that can cause second harmonic signals of background fluorescence. One of these is the interference filter itself as its transmission changes during tilting (Fig. 5.A). The second is the inhomogeneity in excitation light source emission spectrum (Fig. 5.B). Together these phenomena cause a non-linear excitation light intensity changes during wavelength modulation and induce second harmonic fluorescence signal even if absorption within modulation interval $\Delta\lambda$ is constant. Therefore, it is essential to compensate excitation light intensity changes during wavelength modulation.

There are several publications that consider the theory behind interference filter transmission changes [13], but it is more practical to solve excitation light intensity variation problem experimentally than do complex calculations that may not to comply with reality. In our experiment excitation light intensity diminished 63% as we changed incidence angle from $\theta_{min} = 11.5°$ to $\theta_{max} = 27.3°$ (narrow line in Fig. 6). We compensated this variation by regulating output current of excitation light source (Bivar UV5TZ-400-30) power supply (SRS LDC501) with an external voltage applied to its modulation input. This voltage waveform was automatically determined by LabVIEW program. Firstly, it measured and recorded **raw intensity changes** ($\boldsymbol{I_{raw}}$) during wavelength modulation (narrow line in figure 6). Then, keeping the photodiode signal constant and changing LED power supply modulation input voltage during interference filter tilting, program found the **initial LED control voltage** ($\boldsymbol{U_{init}}$) waveform. PID regulator principles were used to optimize and accelerate this process. However, stability of excitation intensity during application of initial control voltage was insufficient. Therefore, a simple correction algorithm was developed and implemented thru LabVIEW program.

The algorithm used the following equation:

$$I_{corr} = \frac{U_{init} * (I_{perfect} - I_{raw})}{(I_{stab} - I_{raw})} \quad \textbf{(22)}$$

where I_{corr} is corrected control voltage, $I_{perfect}$ is theoretical perfectly constant intensity and I_{stab} is measured intensity stabilized by PID control voltage.

It occurred that the time dependence of LED supply control voltage was bell-shaped and could be fitted precisely by a Voigt function. We used it to eliminate the statistical noise of corrected control voltage. Thus we achieved excitation light stability up to 0.5% (bold line in Fig. 6). G.B.Rieker et al. solved excitation light intensity instability problem by normalizing the second harmonic signal (S_2) to the first harmonic (S_2/S_1) [14]. In our case, this was not possible because our lock-in amplifier (SR850 DSP) could not simultaneously measure two harmonics. Our method has the advantage of a constant signal to noise ratio during wavelength modulation.

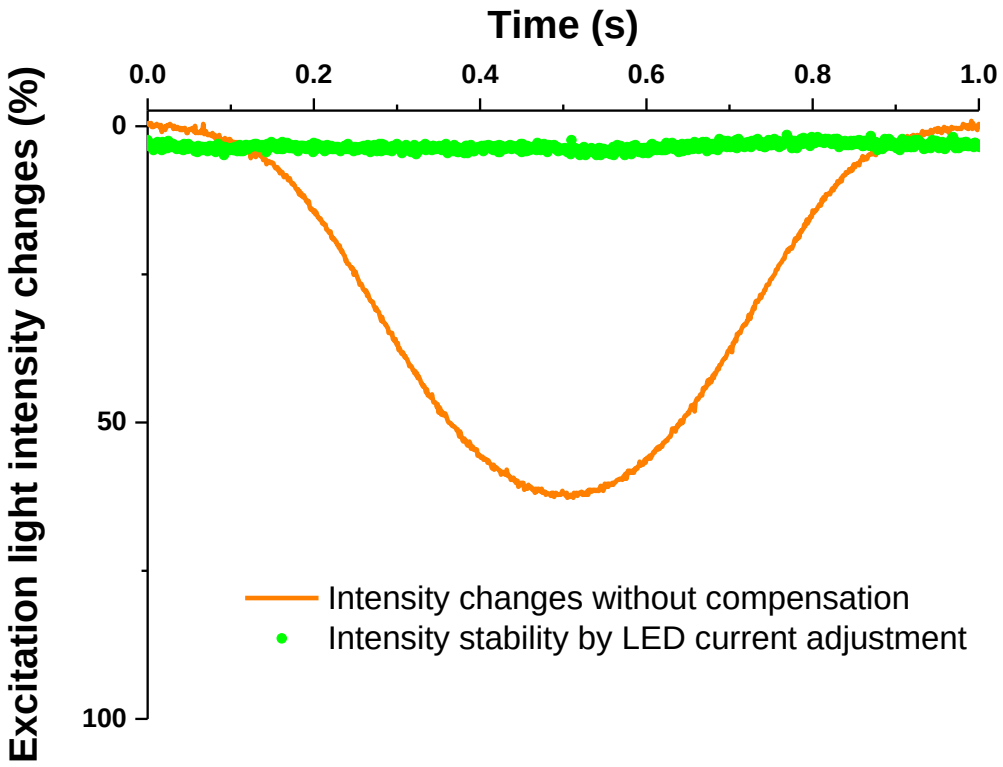

Fig. 6 Excitation light intensity changes during one period of wavelength modulation without (narrow line) and with (bold line) LED current adjustment.

6. Experimental setup and sample preparations

A. Experimental setup

To experimentally test the proposed method, we selected benzo(k)fluoranthene (BKF) as a representative PAH because of its high fluorescence quantum yield. The position of the longest wavelength absorption maximum of BKF is at 399.5 nm, which matches available commercial excitation light sources and interference filters. Schematics of the experimental setup are shown in Fig. 7. An excitation light beam from an ultraviolet LED (Bivar UV5TZ-400-30) is collimated onto a narrow band interference filter (Omega Optics, 405BP3, FWHM = 3 nm, $\lambda_0 = 404.6\,nm$), periodically tilted for wavelength modulation of its transmission band.

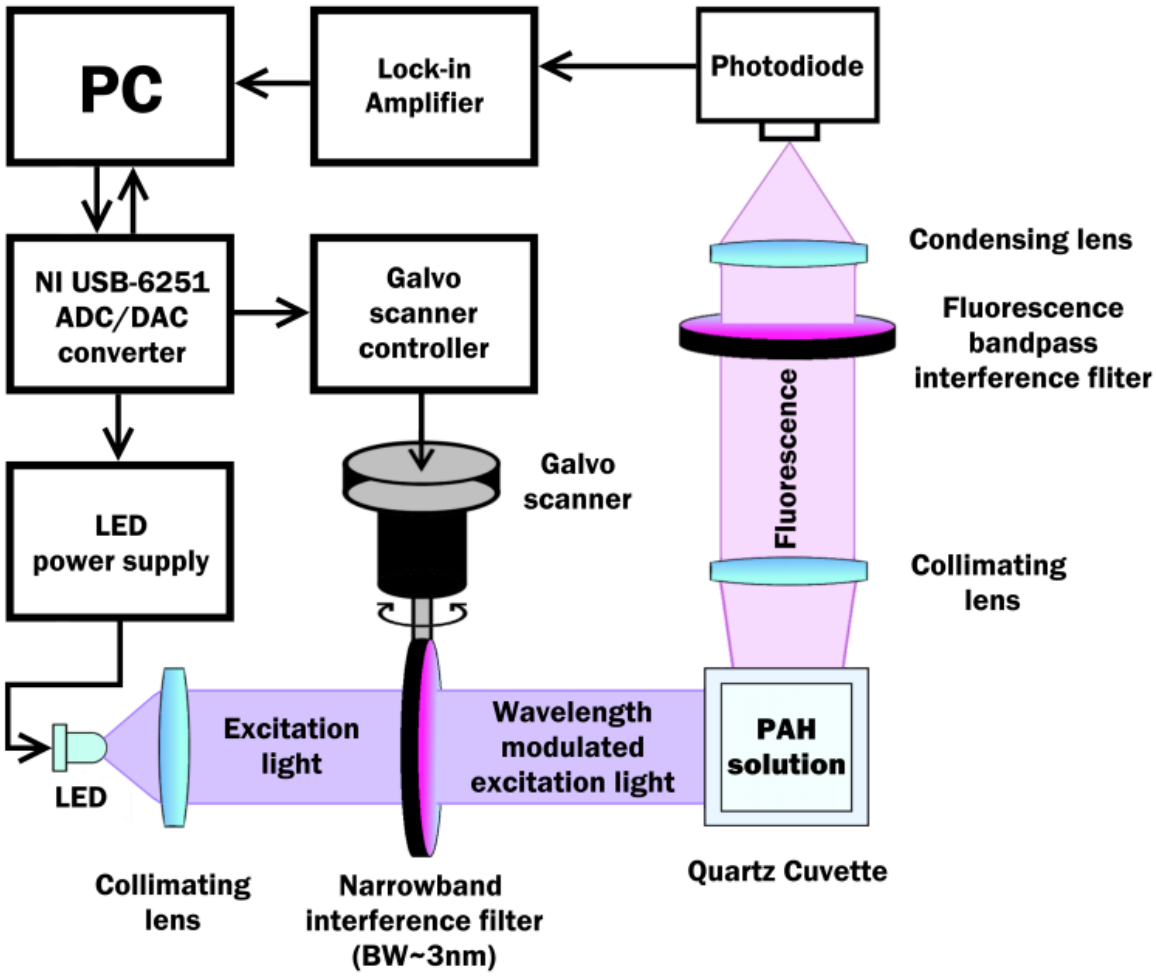

Fig. 7. Experimental setup schematics.

Tilting of the interference filter was performed with a high-speed (20Kpps (kilopoints per second)) optical galvometric scanner (TE-LIGHTING PT-20K). The galvo-scanner control voltage waveform was calculated using galvo-scanner linear transmission function $U(\theta)$ and the equation (13). Calculated control voltage was obtained from analog-digital converter (NI USB-6251) controlled by a LabVIEW program.

As interference filter oscillated the LED current was regulated to compensate excitation light intensity changes. The regulation was done by another LabVIEW program, that automatically found required control voltage and provided it to the LED power supply (SRS LDC501) through NI USB-6251 analog-digital converter.

The resultant wavelength modulated and intensity stabilized excitation light was directed onto the sample within a quartz cuvette with 10 x 10 mm^2 cross section. Fluorescence was gathered at 90 degrees focused with a lens onto the ODA-6WB-500M preamplified photodiode through a D430/30M bandpass interference filter. The photodiode signal was measured at the second harmonic of excitation light wavelength modulation frequency with a lock-in amplifier.

B. Preparation of PAH dilution series

To estimate WMS techniques suitability for PAH detection we prepared a series of benzo(k)fluoranthe solutions from $1 \cdot 10^{-9}\ M$ to $2.30 \cdot 10^{-5}\ M$, diluting an initial solution with concentration of $2.30 \cdot 10^{-5}\ M$. Initial solution was prepared from pure, crystalline benzo(k)fluoranthe dissolved in methanol. The concentration of initial solution was determined using benzo(k)fluoranthene extinction coefficient and absorption spectrum measurements conducted with a Jasco V-570 spectrophotometer. Dilution was performed with the use of Genex beta variable pipettes with volume ranges of 20-200 µl and 100-1000 µl.

7. Results

Several measurements were conducted using the $2.30 \cdot 10^{-5}\ M$ BKF solution. The time-dependent fluorescence signal was visualized by Tektronix TDS 524A digital oscilloscope and compared with the galvo-scanner control voltage (which varies at the modulation frequency ω). For excitation light wavelength modulation around the absorption maximum, the fluorescence signal was, as predicted, at the second harmonic 2ω (panel A in Fig. 8). When wavelength modulation is centered at the upslope of the absorption peak (panel B in Fig. 8), both signals have the same first harmonic frequency. The finite response rate of the photodiode preamplifier (cutoff frequency = 130 Hz) results in the visible phase shift in the fluorescence signals. Lock-in measurements confirmed the second harmonic fluorescence signal prevailing over first harmonic with ratio 6:1 during wavelength modulation around the absorption maximum, whereas first harmonic signal prevailed during upslope modulation.

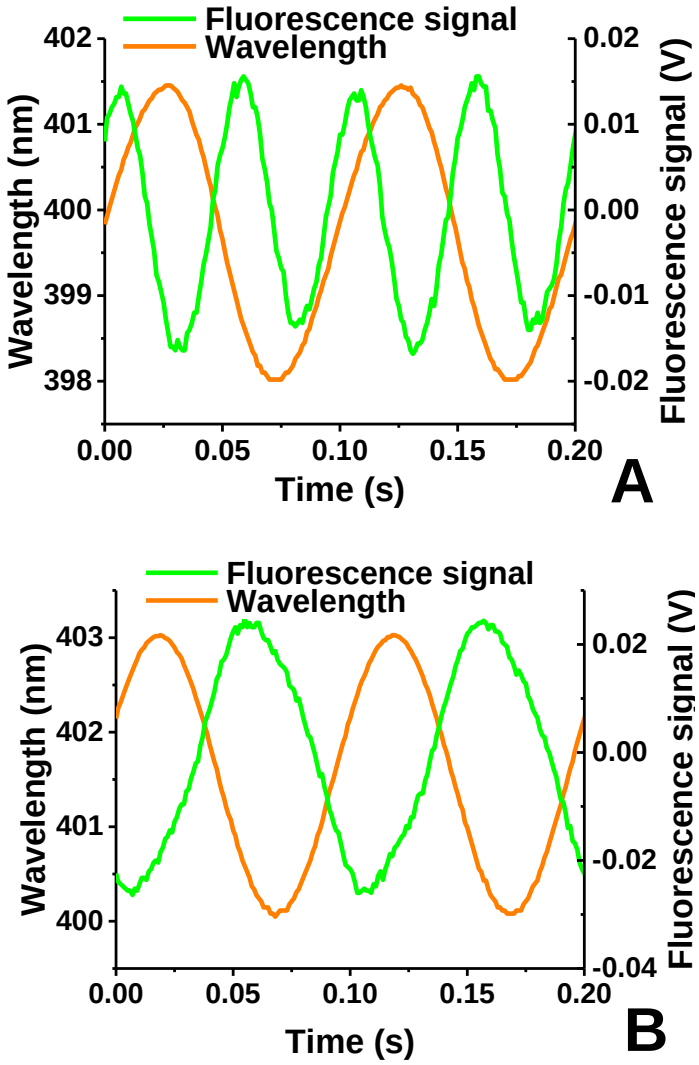

Fig. 8. Waveforms of fluorescence intensity signals during wavelength modulation around absorption maximum (A) and at the downslope of absorption peak (B).

To estimate the sensitivity of WMS techniques for PAH detection we recorded the second harmonic signal by SR850 lock-in amplifier for a series of concentrations ($1 \cdot 10^{-9}\ M$ to $2.30 \cdot 10^{-5}\ M$ mol/L) of benzo(k)fluoranthe solutions (Fig. 9).

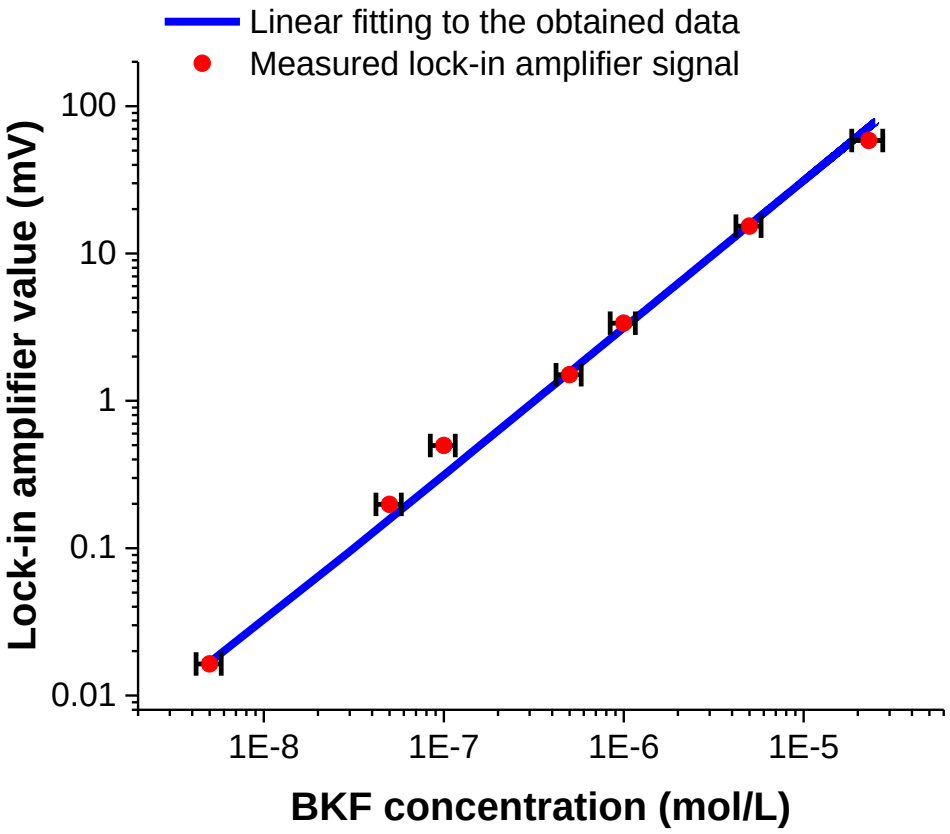

Fig. 9. Measured SR850 lock-in amplifier signal vs benzo-(k)fluoranthene probe concentrations, approximated by weighted linear regression with weighting of $1/x^2$. Data is expressed in log-log scale due to the broad range of concentrations. Error bars show uncertainty of concentrations at a *level* of *confidence* of *95%* (see text for details).

Due to direct proportionality of concentration and fluorescence intensity, we expected also a linear relation between lock-in amplifier signal and benzo(k)fluoranthene concentration changes. To check this hypothesis, we applied a linear regression to acquired data. We used a weighted linear regression because of concentration heteroscedasticity. For the weighting factor, we chose a $1/x^2$ as was suggested by Huidong Gu et al. in the case of direct proportionality between variable and its standard deviation [..]. The obtained linear approximation (Fig. 9) goes through almost all the points, and lies within concentration uncertainties. Only one point deviates significantly from the linear regression line, what is most probably the result of a mistake during sample preparation. The minimum detectable

concentration, we achieved, was $5 \cdot 10^{-9}\ M$. Lock-in amplifier signal for smaller concentrations was indistinguishable from background signal.

The uncertainty of the measurements stems from two basic sources: the sample preparation uncertainty and fluorescence intensity measurement uncertainty. The sample preparation uncertainty originates from Jasco spectrophotometer instrumental error of optical density measurements and from volume measurement uncertainty of Genex variable pipettes. These uncertainties were taken into account and are depicted in Fig 9.

The fluorescence intensity measurement uncertainty results from the finite optical density (OD = 5) of the fluorescence emission filter, which permitted some excitation light bleed-through onto the detector. This resulted in a background signal about 50 μV during lock-in measurements (while smallest measured fluorescence signal is 200 μV), that distorted the fluorescence signal at concentrations smaller than $5 \cdot 10^{-9}\ M$. The SR850 lock-in amplifier instrumental uncertainty is quoted by the manufacturer in the range of 0.2 nV, and therefore should not significantly affect these measurements.

8. Discussion about the results of conducted experiment

The results of the conducted experiments indicate that wavelength modulation spectroscopy can be successfully applied for sensitive PAH detection. Our experience shows that the PAH detection at the limit concentration of $5 \cdot 10^{-9}\ M$ can be achieved. However, we don't see any conceptual obstacles for diminishing this detection limit even further.

The detection limit concentration corresponds to a signal of 0.2 mV. The minimum signal, which can be measured with SR850 lock-in amplifier, is 0.2 nV at low-pass filter bandwidth of 10 mHz (corresponding to a time constant of 10s). This indicates that, in respect of sensitivity of electronic equipment, several orders of magnitude lower concentrations could be detected.

In our case it couldn't be achieved due to imperfection of our experimental system. As we found out, used fluorescence filter optical density at excitation light wavelengths wasn't high enough and caused excitation light leakage. This resulted in a high background during lock-in measurements, that distorted the fluorescence signal at concentrations smaller than $5 \cdot 10^{-9}\ M$. Also due to excitation light residual intensity modulation (remained after intensity stabilization) at level of 2-4% contained higher harmonics, we weren't able to filter excitation light leakage with the lock-in amplifier at second harmonic frequency. In principal, the intensity stabilization of higher accuracy could be achieved, if we would build a feedback system to control LED current instead of calculating control voltages. Or if we could implement normalization of second harmonic signal by first harmonic signal within the lock-in amplifier. Of course, implementation of fluorescence filter with a steeper cut-on edge and higher optical density will also diminish background leakage.

9. Development of BKF sensor prototype based on proposed method and further experiments

The research on application of wavelength modulation techniques for PAH detection was only a part of greater project financed by Environmental Investments Centre (Keskkonnainvesteeringute Keskus). The project goal was to develop a PAH sensor prototype that would be possible to use for on-line water monitoring and sensing of PAHs contamination around concentrations established by European Commission.

The development of the prototype was a complex task. It comprised of optical system design, selection of appropriate electronic hardware and microcontroller, development of software and different kind of testing. All tasks were done step by step and resulted in a working PAH sensor prototype.

A. Optical system design

We started our development by the most crucial part of the sensor – optical system. We took the scheme (Fig 7.) that we used during experiments for the basis and tried to optimize it and achieve the detection of smaller concentrations of PAHs. We tried to increase the efficiency of excitation light focusing on a sample and enhance the effectiveness of fluorescence signal collection from excited area to the photodiode. At the same time, we looked for a simple and compact solution. However, additional restriction was imposed: now, when the detector should be able to work in on-line mode, we couldn't place a sample into a cuvette, but should use a vessel, where the sample (i.e. water) is flowing through. Such demand didn't allow us to place excitation and fluorescence optical paths under 90^{o} degrees to each other as it was done during experiments (Fig 7.). Previously this design was implemented to improve signal to noise ratio by reducing excitation light bleed-through due to its reflections from sample surface.

Therefore, we tried to maintain separation of the different light paths implementing the first possible design that can be seen in Fig. 10. However, after we tested it more thoroughly, using optical elements available in laboratory, we found out that this solution imposes the limitations on fluorescence collection lens diameter and aperture number. It is hard to place a large fluorescence collection lens in a position shown in Fig. 10. and experiments showed, that the area from which the collection of fluorescence is performed, is too small and a resulting signal is too weak for a sensitive detection of ultra-low concentrations of PAH ($< 1 \cdot 10^{-9}\ M$). Therefore, another optical design was considered.

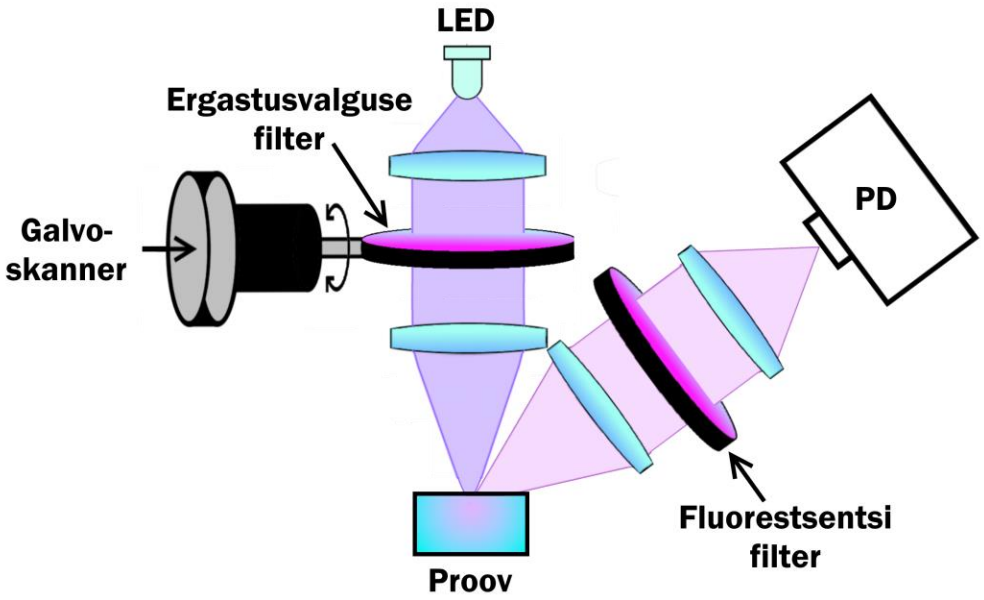

s

Fig. 10. The first tested optical system design where excitation light path and fluorescence collection path are separated. PD stands for photodiode.

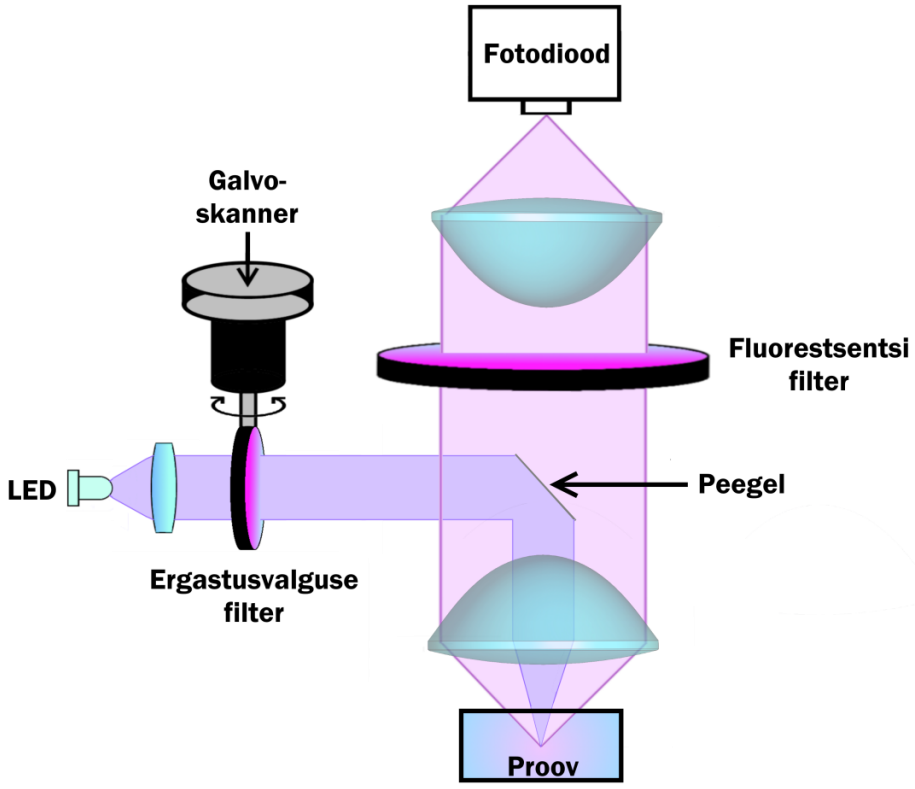

Fig. 11. The second tested optical system design where excitation light path and fluorescence collection paths coincide and the same lens is used for excitation light focusing and fluorescence collection.

The second solution abandoned the separation of different optical paths and used the same lens with great aperture number to excite sample and collect fluorescence (Fig. 11). The excitation light was directed from the side onto a mirror placed under 45 degrees at the system optical axis, which reflected excitation light onto the focusing lens. Lens focused the light onto the sample and at the same time collected the fluorescence from exactly the same point. Due to large aperture number a lot more fluorescence was collected. Fortunately, the excitation light bleed-though, caused by reflections, increased insignificantly compared to the fluorescence signal and overall signal-to-noise ratio improved enabling detection of ultra-low concentrations of PAH ($< 1 \cdot 10^{-9}\ M$). We believe that it happened due to the mirror placed on the way to the photodiode.

The system also became more compact and simple. Moreover, it didn't require many custom components, while most of them could be obtained from Thorlabs optomechanical company. This was checked by SolidWorks program, where we draw a virtual model of an optical system comprised from Thorlabs products' models. As you can see in Fig. 12, the whole system can be build using commercial products, what is really cost-efficient. For the first solution we designed custom components using SolidWorks and attempted to 3D print them, but the precision of 3D printer was insufficient and we couldn't produce components of required quality. That put an end of design selection and we stopped on the second variant of optical system design.

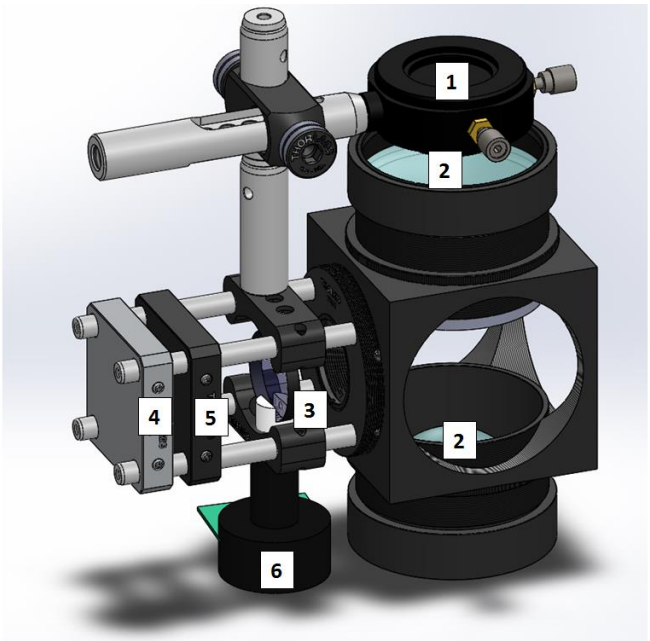

Fig. 12. PAH sensor optical system model drawn in the SolidWorks program. 1 is a photodiode holder, 2 are aspherical lenses, 3 is narrow-band interference filter, 4 is part for the LED mounting, 5 is a possible LED collimating lens mount, 6 is galvoscanner used in experiments and attached to the system using Thorlabs components.

When the design was set, we continued enhancement of the system by selecting more efficient optical components. First of all, we focused on excitation light source. It is easy to understand that if we use more powerful excitation light source, we get stronger fluorescence signal. And if the increase of excitation light bleed through fluorescence filter is less significant than fluorescent signal enhancement, we improve signal-to-noise ratio. Therefore, we changed low-power Bivar UV5TZ-400-30 UV-LED that we used in experiments to a superior high-power excitation light source - Nichia SMD LED UV NCSU275. It has spectral maximum at 395±3 nm, 20 nm FWHM and can reach the power of 370 mW. Although we didn't require such amount of excessive power, it allowed us to find optimal power mode (~40 mW) by selecting appropriate LED current. Other available UV-LEDs were too weak or too powerful. Also, for efficient excitation light collimation it was important to have a light source close to spot light source. So selected LED should have a small light emitting area besides high power. New Nichia UV-LED provided had this required feature.

Secondly, we considered excitation light collimation lens. To efficiently direct excitation light onto a mirror (Fig. 11) and then onto the sample, we required a strong lens with great aperture number to collect and collimate as much excitation light as possible. At the same time, we wanted to keep system as compact as possible. This means, we had to find lens with the small diameter and great aperture number. For this reason, we tried two options. First was the use of combination of two 1 inch lenses available in the laboratory. Combined they gave the lens with numerical aperture about 0.8. They gave a satisfying result but weren't the most compact solution, so we bought from Thorlabs company a ½ inch aspherical lens with aperture number 0.78. Unfortunately, its area was too small for the selected light source and collimation was inefficient – we couldn't treat a LED as a spot light source anymore. Therefore, we stayed with the first solution as we couldn't find any better commercially available lenses.

Thirdly we thought about excitation light focusing and fluorescence collecting lens. For the sake of a compact solution, we again required lens with great numerical aperture. We tried to use lenses available in laboratory and their combinations, but couldn't reach satisfying result. So, we ordered 2 inch ACL50832U-A aspheric lens from Thorlabs company. It had numerical aperture of 0.76 and satisfied our expectations. It is also important to mention, that due to the design of the system we couldn't afford focusing/collection lens with small diameter, as the design can be efficient only if mentioned lens will have diameter significantly greater than excitation light directing mirror. Otherwise, the fluorescence signal will be to weak. The was just the right size this case, as its effective area was 4 times greater than the mirrors and 75% of fluorescence was collected. For the collected fluorescence focusing onto the photodiode we also selected ACL50832U-A Thorlabs lens as it we couldn't find any better commercially available solution. Also all the mentioned lenses had antireflection coating and were made from B270 Optical Crown Glass that transmitted UV/blue light in required region (350-460 nm)

The wavelength modulation part remained the same. We couldn't find any better interference filter than we already had and galvo-scanner produced the best modulation precision (Fig. 4). The fluorescence filter also was already well-chosen (Edmund Optics 440nm CWL, 40nm BW, OD 6). However, we required a version compatible with the new design, i.e. with greater diameter. Therefore, we ordered it from Edmund Optics company. For the fluorescence detector we used ODA-6WB-500M photodetector with built-in operational amplifier and enhanced sensitivity in blue light region. Construction elements and lens holders were ordered from Thorlabs. Finally, we assembled the sensor optical system from all selected components (Fig. 13, 14). Test showed that designed system enabled detection of ultra-low concentrations of PAH ($< 1 \cdot 10^{-9}\ M$).

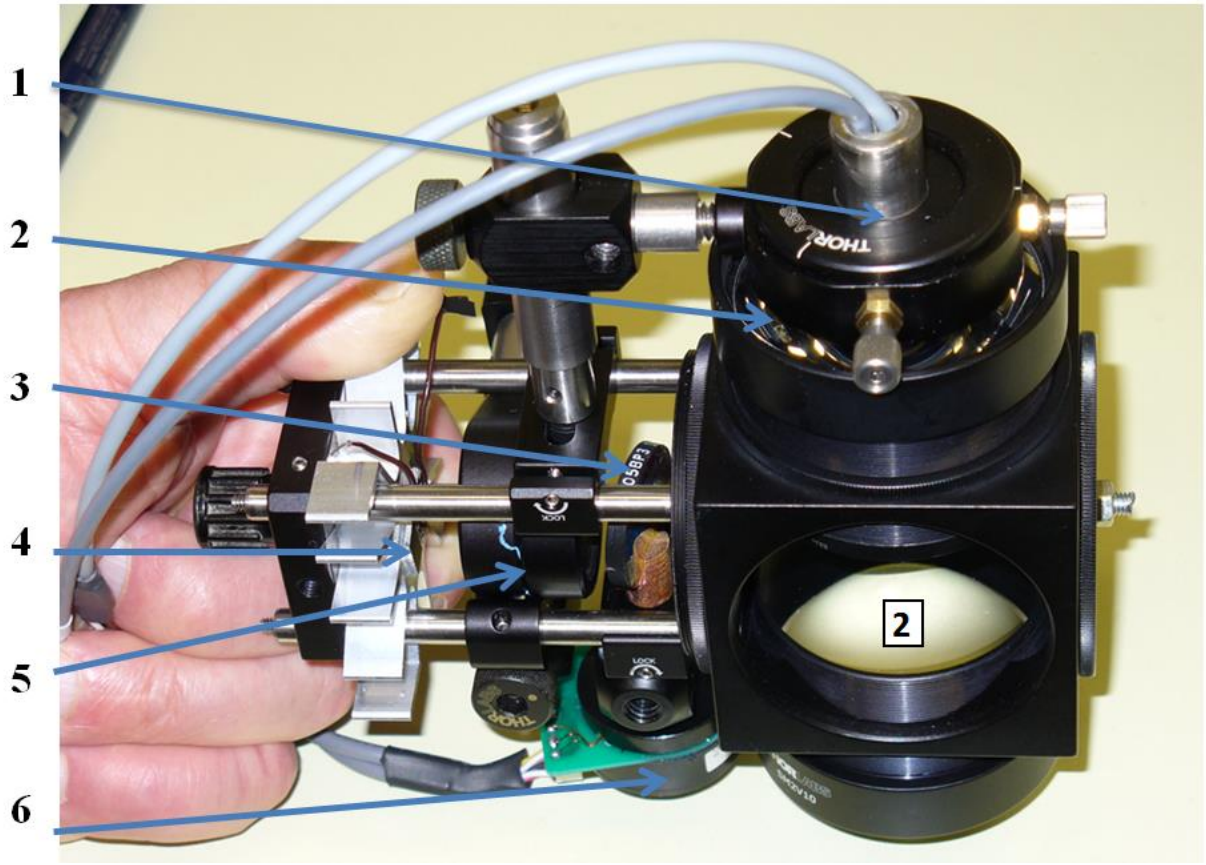

Fig. 13. PAH sensor optical system. 1 is a photodiode holder, 2 are aspherical lenses, 3 is narrow-band interference filter, 4 is LED on a mounting with a radiator, 5 is a LED collimating lens, 6 is galvoscanner attached to the system using Thorlabs components.

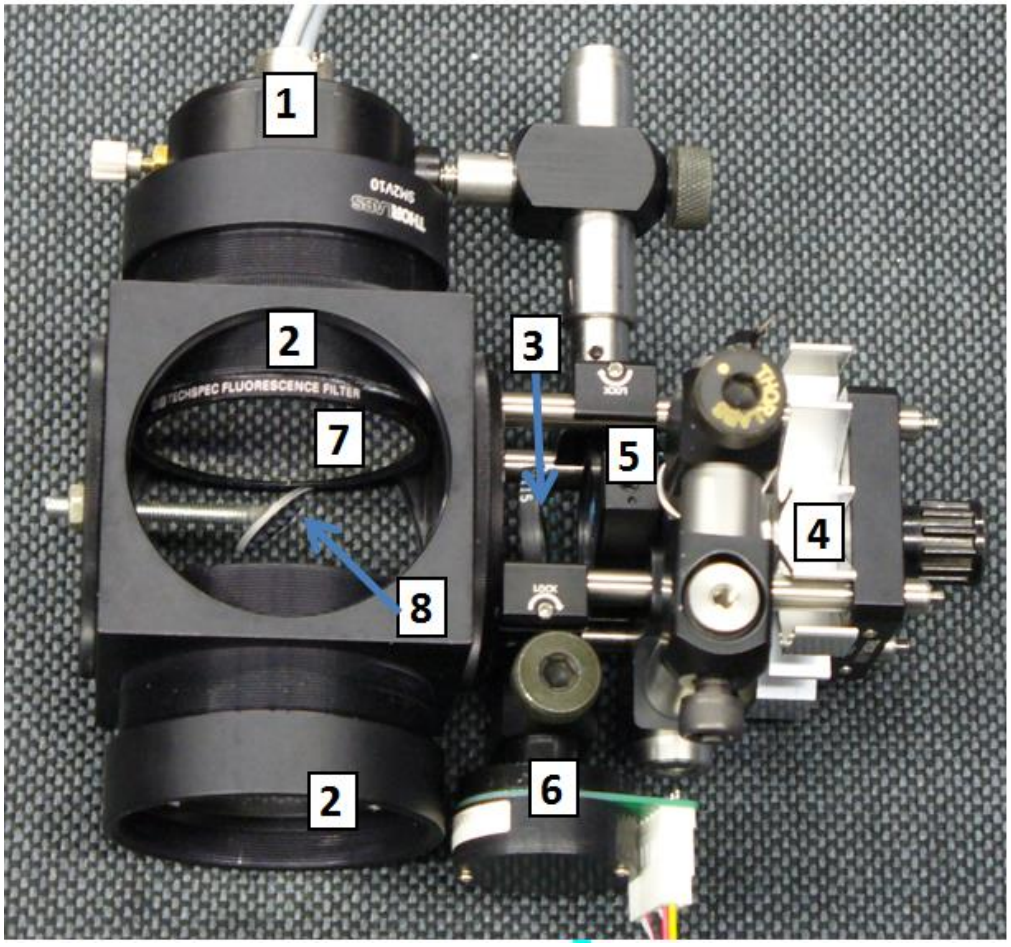

Fig. 14. Another view on PAH sensor optical system. 1 is a photodiode holder, 2 are aspherical lenses, 3 is narrow-band interference filter, 4 is LED on a mounting with a radiator, 5 is a LED collimating lens, 6 is galvoscanner attached to the system using Thorlabs components, 7 fluorescence filter and 8 is an excitation light directing mirror.

B. Selection of electronic components and microcontroller

Microcontroller and hardware selection was a very important task. Previously, during our experiments we used three different high-quality scientific instrumentations: SRS LDC501 – laserdiode controller, SR850 lock-in amplifier and NI USB-6251 analog-digital converter. These instruments allowed to achieve excitation light wavelength sinusoidal modulation, compensation of excitation light intensity changes and sensitive fluorescence detection at the second harmonic of the wavelength modulation frequency. But the developed PAH sensor electronis should be able to provide same or similar capabilities within only one single instrument. That raises serious challenge. Luckily, we can call modern technologies to our aid.

As was already mentioned, the wavelength modulation mechanism remained the same as in previous experiments: interference filter tilting by galvo-scanner TE-LIGHTING PT-20K. However, now we required a signal to drive this module instead of SRS LDC501. That imposed the first selection criteria to PAH sensor hardware: it should be able to generate galvo-scanner control voltage of custom waveform. Secondly, our optical system design didn't include feedback for excitation intensity stabilisation due to requirement for compact and simple solution. Therefore, PAH sensor hardware should compensate light intensity changes in the same way as it was done before or have reasonable alternative. Same goes for fluorescence detection: hardware system should either have built-in lock-in amplifier or any other possible means for frequency-sensitive signal detection.

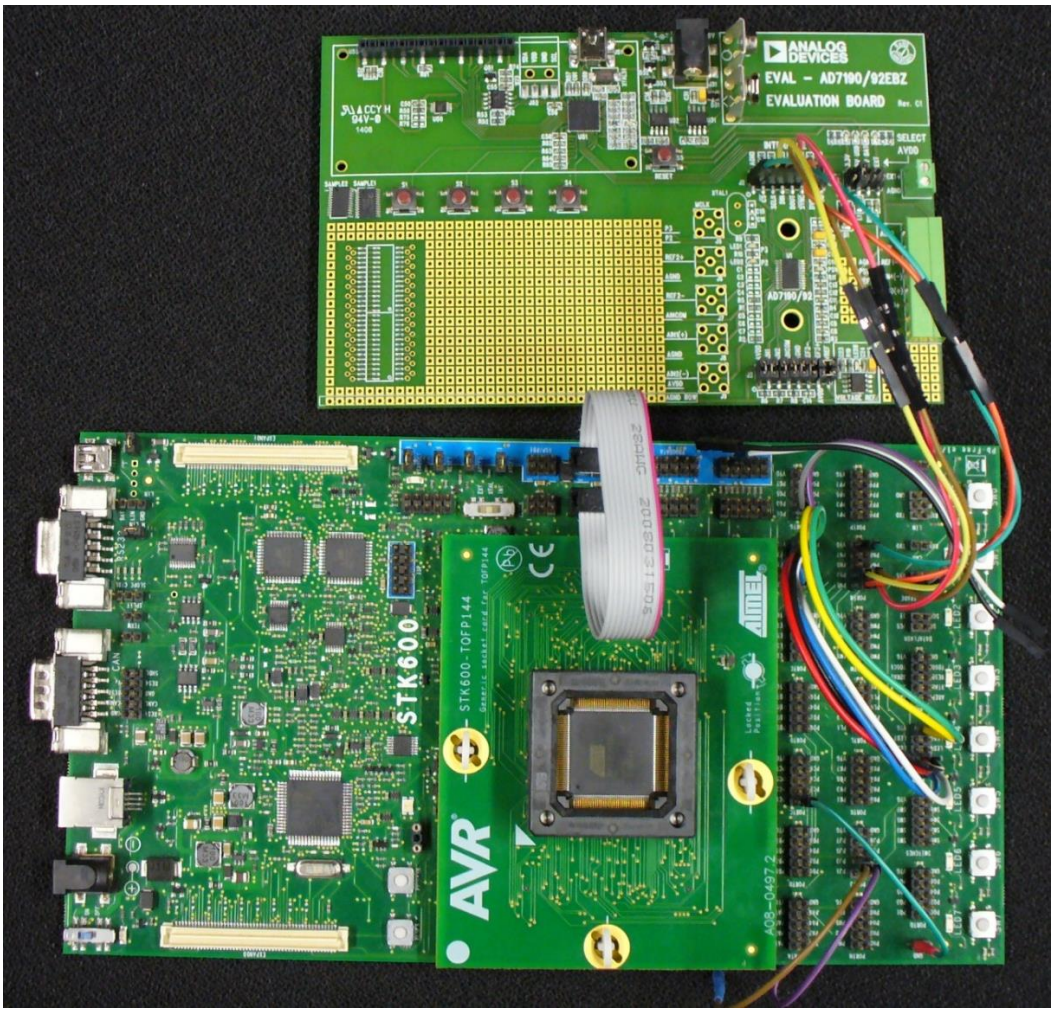

Fig. 15. Atmel AT32UC3C0512C microcontroller on development board STK600 (below) and Analog Instruments AD7190 analog-to-digital converter on the EVAL-AD7190 evaluation board.

We found a fairly good solution in the face of Atmel AT32UC3C0512C microcontroller (Fig. 15). Firstly, it has several built-in 12-bit digital-to-analog (DAC) convertors for signal generation any kind of waveforms. Secondly, it is able to conduct different digital signal processing operations including numerical Fourier transformation of the measured signal. The only thing it lacked, was a good analog-to-digital (ADC) converter for fluorescence signal digitalization. Built-in 10-bit converters were too rough for precise detection. We solved this problem by external noise-free 24-bit Analog Instruments AD7190 analog-to-digital converter (Fig. 15). The above mentioned excitation light intensity changes compensation was possible to achieve using one of 12-bit DAC for generation of LED control voltage. However, for the sake of simplicity, we changed the method and compensated excitation light intensity changes by dividing digitalized fluorescence signal by digitalized curve (Fig. 6, orange line) of intensity changes measured beforehand. Frequency-sensitive detection was reduced to computation of Fourier transformation of measured fluorescence signal.

We bought above-mentioned devices together with development/evaluation boards. That way we didn't need to spend our time for custom PCB development and could use commercially available solutions directly in our prototype.

Another challenge arose from our desire to build fully autonomous device that could work in the field conditions where electricity is not available, i.e. it could autonomously take probes somewhere on the riverbank near potential PAH pollution source and monitor the situation for some time. Therefore, we required a complex power supply system, that could provide required power to all PAH sensor electronic components from some kind of rechargeable batteries/accumulators. As the combination of system components is unique and all different components required specific voltages, the commercially available ready-to-use solution for this problem doesn't exist. That is why we asked for help from Agu Anijalg and developed our own custom power supply solution. It uses Fennel PWP-250W/P6Y-250 solar panel of 250W power to charge 30V Li-ion accumulator, which voltage is then converted to required voltages by universal DC-DC convertors. The appearance and schematics of this system can be seen in figures 16 and 17.

However, for full autonomy, PAH sensor required also an automatic sampling mechanism, which development was fairly simple task and we easily found solution. Basically, we integrated into the system a pump and electronic valve, which were connected to the power supply system and could be controlled by a microcontroller.

Finally, for the convenient data acquisition, the microcontroller PCB was extended by WiFi module, that allows system to connect to internet and send logged measurement data to the end user. That way we achieved to design system capable for fully autonomous detection of small concentrations of PAHs.

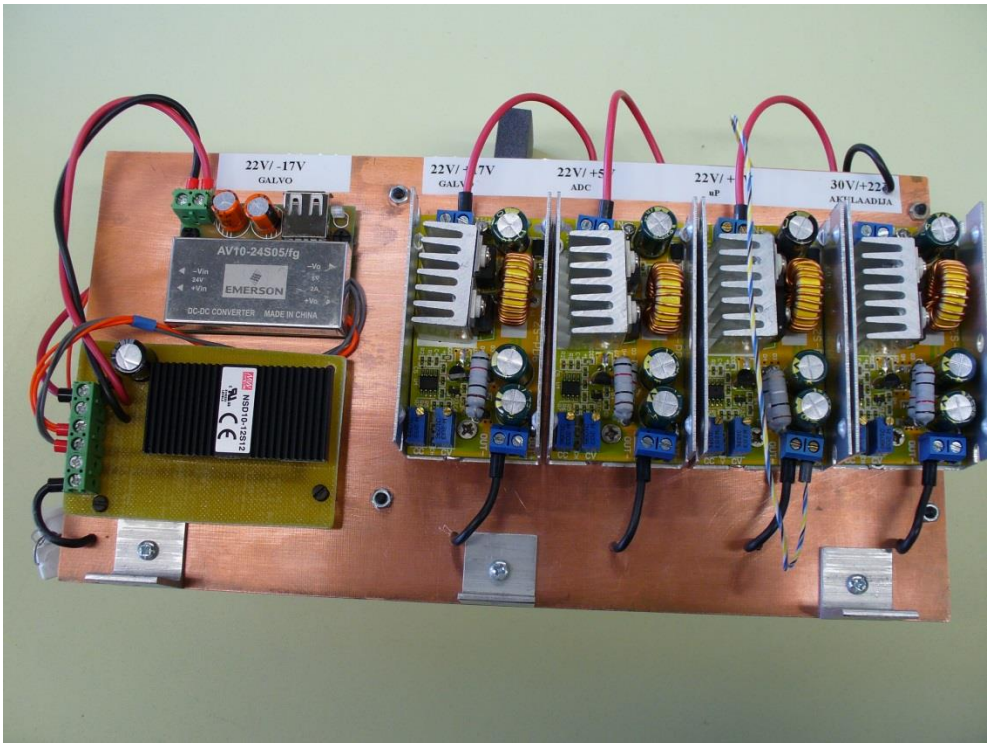

Fig. 15. Custom power supply board.

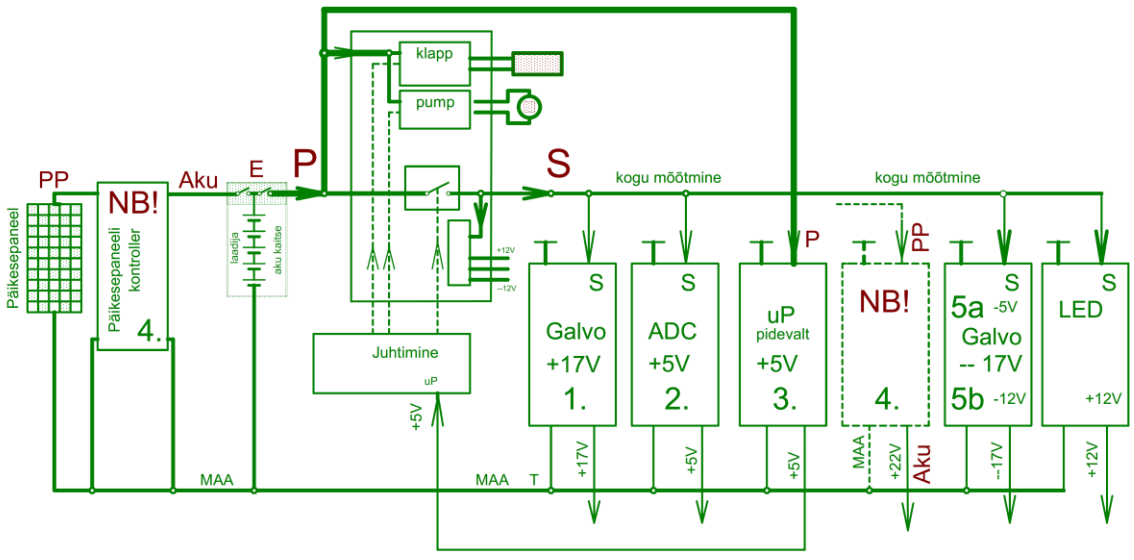

Fig. 15. Custom power supply schematics.

C. Development of the sensor software

Last but not least stage of the PAH sensor prototype development was the software development. Our goal was to bring to life all the hardware components and make them work together for the sake of selective and sensitive detection of PAHs. For this reason, we wrote several different programs for Atmel AT32UC3C0512C microcontroller and user interface for PC.

Programs for microcontroller were written in C programming language using Atmel Studio Integrated Development Environment (IDE) (Fig. 16). Atmel IDE usage significantly reduced the time of software development and simplified use of compilator.

The first program controls sample acquisition. It uses AT32UC3C0512C digital outputs to switch on and off system's pump and electronic valve. It was decided to use periodical sampling mode, when pump fills the sampling vessel with the sample, measurement is conducted and then system opens valve discarding measured sample. Of course, we could just make the sample (potentially polluted water) flow through the system, but this case is energetically inefficient as pump will continuously consume system energy stored in Li-ion accumulator. Periodical sampling put sampling mechanism on standby saving the system energy. Period of sampling cycle was determined by duration of single measurement.

Measurement control program is more complex. It starts when sample vessel was filled and first of all it switches on excitation light source and galvo-scanner using microcontroller digital outputs. Then it starts 12-bit DAC, loads control voltage digital array and starts generation of interference filter tilting waveform that produces sinusoidal excitation light wavelength modulation. Next, program connects with external 24-bit AD7190 ADC connected with the photodiode via SPI interface and starts fluorescence signal acquisition. It digitalizes and saves fluorescence intensity changes occurred during 16 periods of interference filter tilting. Such amount of periods is required to enhance resolution of frequency scale of Fourier transformation applied to the signal in the next program stage. But before that acquired fluorescence signal is divided by excitation light intensity changes waveform loaded from the microcontroller's memory. Such procedure eliminates the contribution of excitation light intensity changes to the signal at the second harmonic of wavelength modulation. When the Fourier transform is done the system normalizes obtained power spectrum and sends it to the PC interface program via wireless internet connection or cable. Optionally system can send only measurement result, but during system tests spectrum was more informative. Finally, system switches off galvo-scanner and excitation light source sending a signal to empty sampling vessel.

Third program is responsible for communication with external devices. It provides connection to the PC via WiFi or RS-232 cable, allows to receive external commands and sends responses or inquired information. Command syntax is preprogramed within this program and corresponds to abbreviations of commands. Such mechanism is required to conveniently change sensor operational modes, test

modes and settings. For example, it allows to trigger the recording of the new excitation light intensity changes waveform if necessary, switch operation to ADC test or send command to calculate and rewrite galvo-scanner control voltages. It is also possible to switch off Fourier transform and send raw fluorescence intensity data that could be analysed afterwards using other methods. In fully autonomous mode, the system can be ordered to analyse Fourier spectra (i.e. follow the signal only at the second harmonic of wavelength modulation) and send a warning or emergency signal if PAH concentration exceeds a preprogramed level. For each of the modes a separate function or program is written. They either implement equations described in the beginning of this work or implement slightly modified programs described above. Galvo-sacnner control voltages, for example, are calculated using equation 19. ADC test just switches off Fourier transform and signal division and sends directly ADC measurement results. Fluorescence measurement leaves division by excitation light intensity changes waveform. Fully autonomous mode just extends a bit normal mode calculating average around measured Fourier power spectrum peak and comparing it with a single value. Recording of the new excitation light intensity changes waveform can be done when photodiode is place to the position of the sample so the excitation light intensity is measured instead of fluorescence. It implements a standard "fluorescence" measurement program without any transforms and divisions and records the result to memory.

Finally, we wrote a main microcontroller program that initialized microcontroller and external ADC systems and put all other programs together. When PAH sensor system is started it first of all starts main program that puts system on a standby and activates communication program that waits for external commands. When command is send, communication program delegates operation to the other program that corresponds to sent command. Communication program sends answers or data and continues to monitor any other incoming commands so we can easily stop PAH sensor operation by sending stop command or we can change operational mode.

PC user interface was written using LabVIEW visual programming environment. It was chosen because it allowed quickly and easily create decent graphical design (Fig. 17). The interface program connects to the PAH sensor via RS-232 cable or WiFi and allows to send command to AT32UC3C0512C microcontroller. Afterwards it receives the answer or inquired information. If measurement data is sent, interface program plots it on a graph allowing data analysis. It is also possible to change data visualisation style and save inquired data. Therefore, PC interface program provides all necessary functions for convenient and successful PAH sensor application.

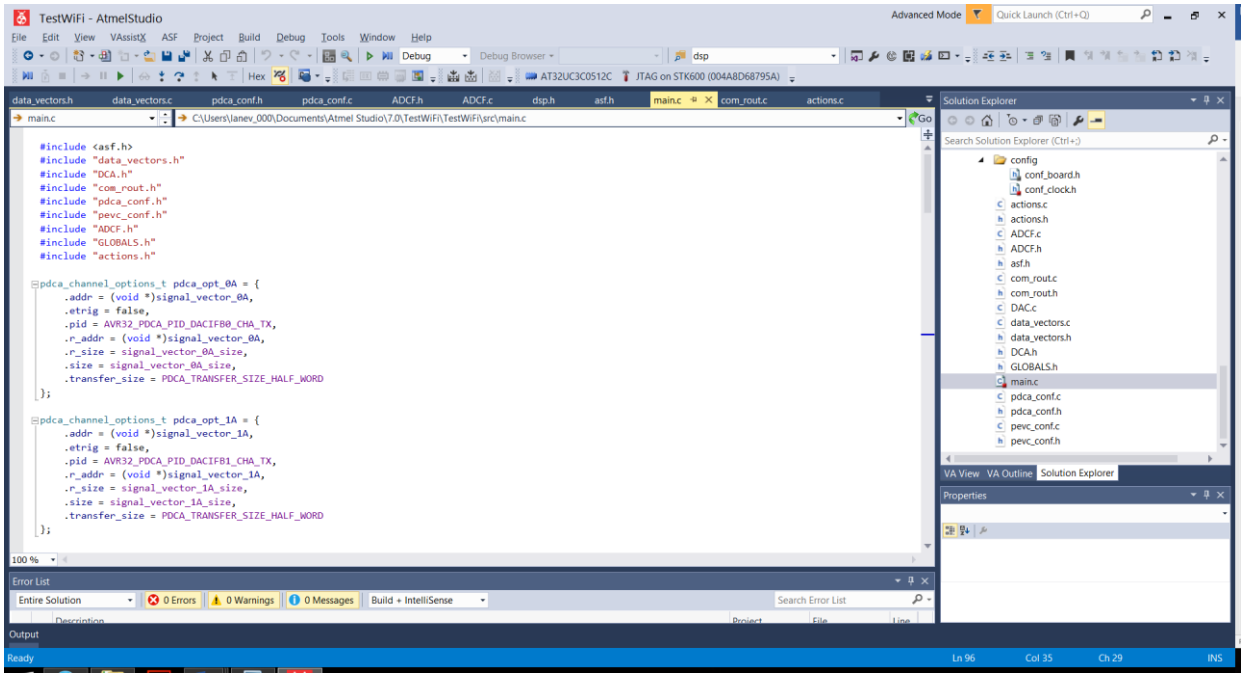

Fig. 16. Atmel Studio IDE and fragment of the main program.

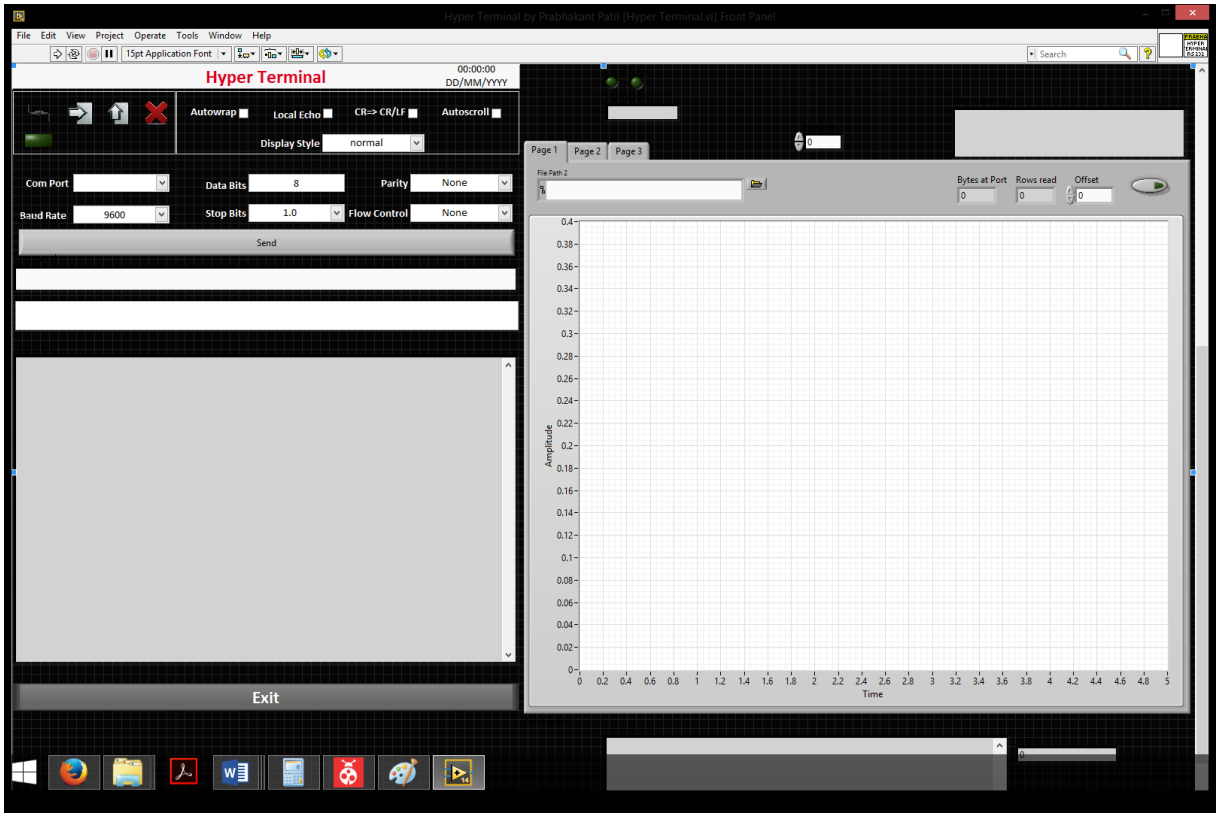

Fig. 17. PC interface program graphical design made in LabVIEW graphical programming environment.

D. Assembly of the prototype

When the development of optical system, selection of hardware and programming were completed, we assembled the system. For this reason, we bought a metal box of required size, made custom mounts and connected all components together. The result can be seen in figure 18.

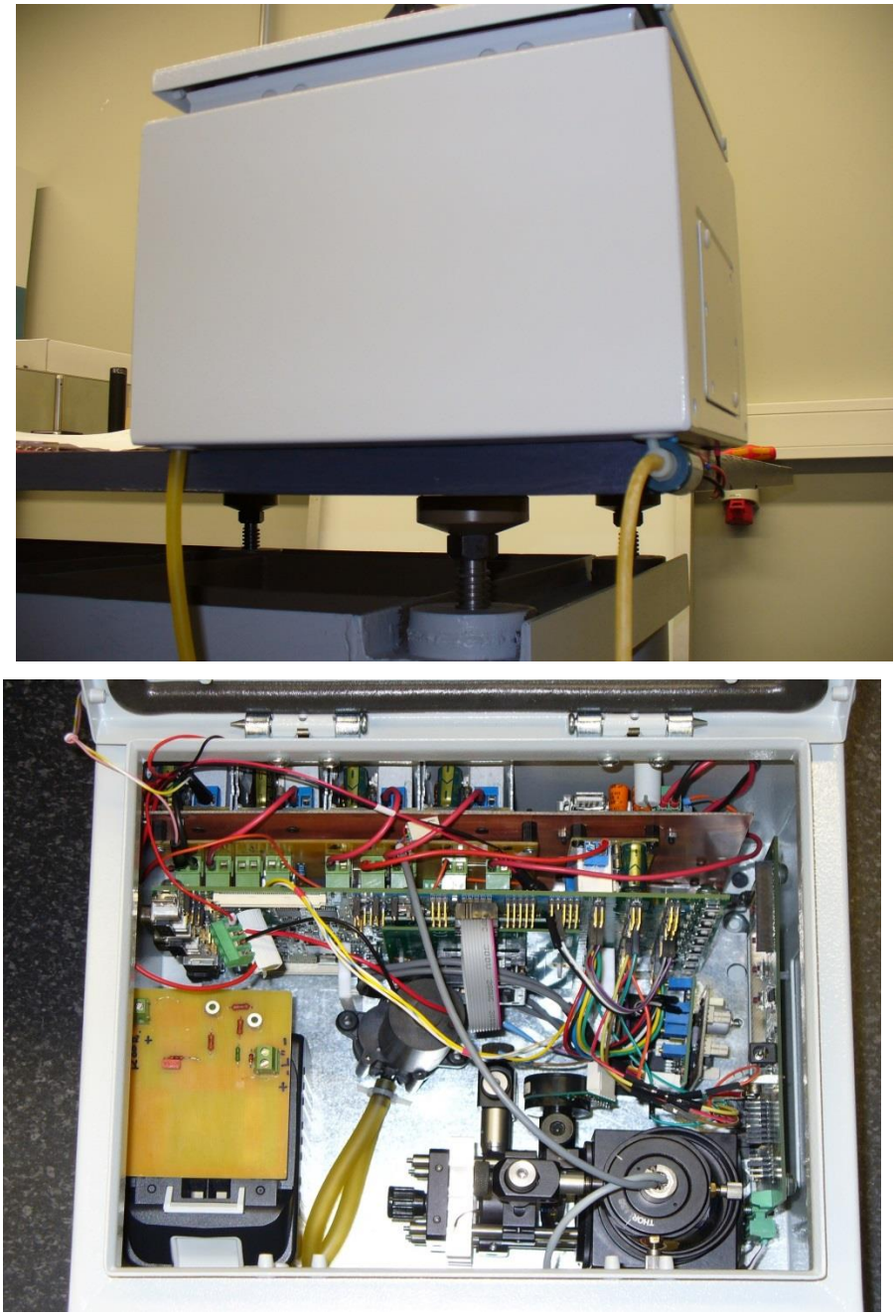

Fig. 18. PAH sensor prototype final assembly.

10. Prototype testing and experiments with the water

To test the actual performance of the developed prototype we conducted several experiments. First of all, we measured the Benzo(k)Fluoranthene solution of smallest concentration ($5 \cdot 10^{-9}\ M$) that we could detect before. The PAH sensor successfully detected BKF in the sample. We also found out that due to system optical design, the fluorescence signal strength increased 4.5 times. This allowed us to detect even 10 times smaller concentration than before - we could detect 0.5 ppb ($5 \cdot 10^{-9}\ M$). The corresponding sample solution was obtained by dilution of $5 \cdot 10^{-9}\ M$ BKF solution.

Next, we tried to depart from the ideal conditions and conducted an experiment with the mix of BKF solution and sewage water sample obtained from Tallinn water treatment company "Tallinna vesi". For sample preparation we used initial $2.30 \cdot 10^{-5}\ M$ BKF solution. We diluted it by sewage water so that we obtained solution of $2.3 \cdot 10^{-6} mol/L$. We also prepared a control BKF solution in methanol with the same concentration. Dilution was used, because we didn't have BKF crystals in laboratory anymore to make new solution in water. High concentrations of BKF were used to obtain illustrative absorption spectra of prepared solutions and sewage water that we measured using Jasco V-570 spectrophotometer. The result is depicted on figure 19. The water contained seaweeds, bacteria and other organic substances that gave fluorescence background, which as expected was similar to the linear background. The absorption spectrum of the mix of BKF solution and water corresponded to the sum of absorption spectra of pure BKF solution in methanol and "pure" sewage water, as expected.

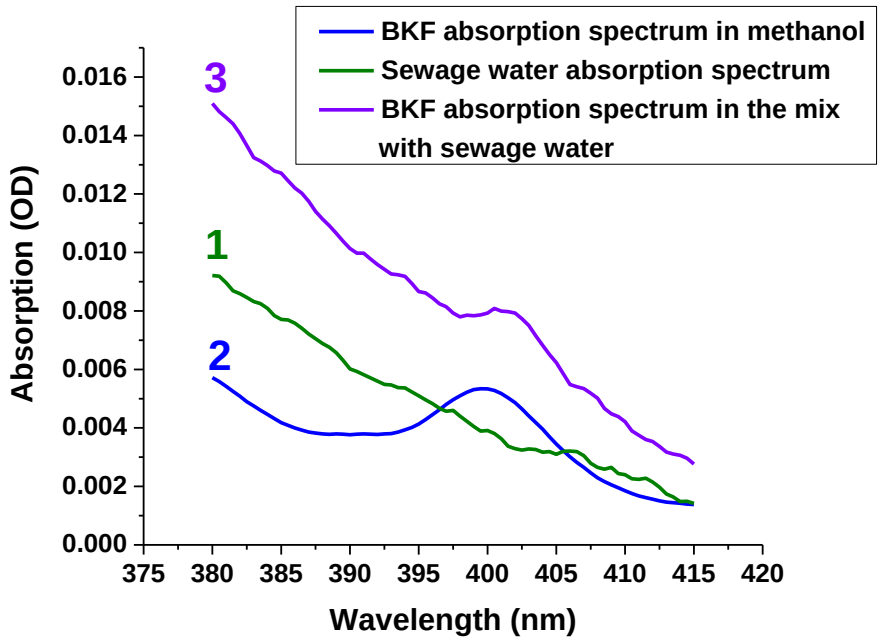

Fig. 19. Absorption spectra of BKF solution in methanol (2), sewage water (1) and mix of this substances (3).

When the sample solutions were prepared, we ran them through developed PAH sensor prototype and conducted measurements, obtaining Fourier transform power spectra shown in figure 20, where are also depicted the waveform of periodic fluorescence signal obtained during excitation light wavelength modulation, which in our case was 1 Hz.

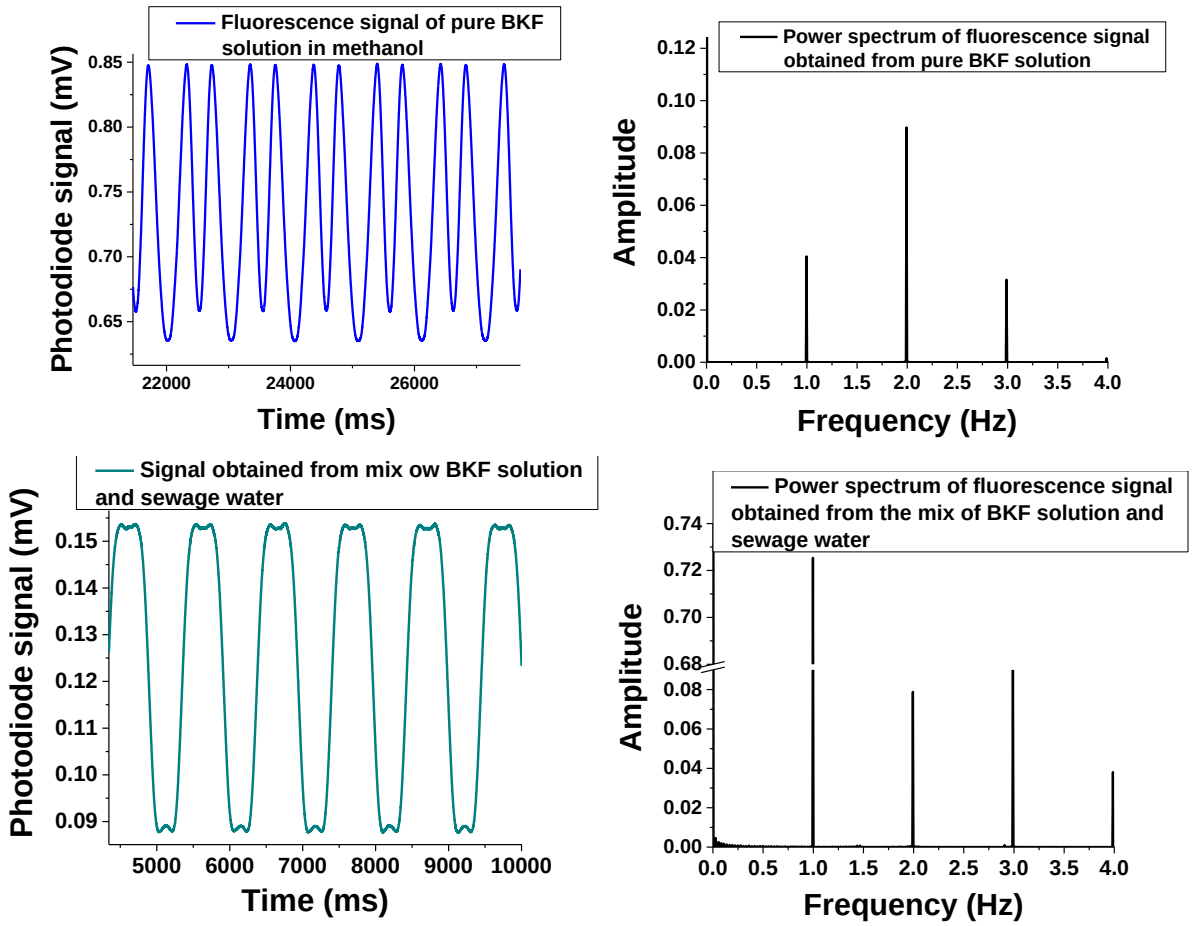

Fig. 19. Periodic fluorescence signal waveforms obtained during excitation light wavelength modulation (left) and Fourier transform power spectra obtained as a result of PAH sensor test measurements (right).

As we can see, the power spectra peaks, located at the second harmonic of wavelength modulation (2 Hz), have very similar maxima values (0,089 ja 0,079), while the other power spectrum components differ significantly. The first harmonic component of the BKF solution mix with water is about 18 times stronger. This means that using PAH sensor prototype, based on excitation light wavelength modulation, we can selectively sense PAH (in this case BKF) separately from the other substances. That proves the efficiency of interference filter tilting and excitation light wavelength modulation for detection of polycyclic aromatic hydrocarbons.

11.Conclusion

Sensitive detection of the polycyclic aromatic hydrocarbon benzo(k)fluoranthene by application of the WMS method has been realized. The sensitivity and selectivity is achieved by detection of the second harmonic 2ω of the fluorescence signal under sinusoidally modulated (at frequency 1ω) excitation wavelength around the narrow absorption peak. The sinusoidal excitation wavelength modulation was achieved by precisely tilting a narrowband interference filter in the excitation light path. The prototype of PAH sensor based on proposed wavelength modulation method and capable for PAH on-line detection was developed and tested. Tests proved the high selectivity and sensitivity of proposed method. We were able to detected benzo(k)fluoranthene to a concentration limit of $0.5 \cdot 10^{-9}\, M$.

12. References

1. United States Environmental Protection Agency, "Polycyclic Aromatic Hydrocarbons" (Office of solid waste, Washington, DC, January 2008).

2. European Commission, "Polycyclic Aromatic Hydrocarbons – Occurrence in foods, dietary exposure and health effects" (Health and Consumer Protection Directorate, Scientific Committee on Food, Brussels, Belgium, 2002).

3. European Commission Regulation No 1272/2013, OJ L 328 (2013), p. 69–71.

4. World Health Organization, "Polynuclear aromatic hydrocarbons in Drinking-water", 2nd ed. Addendum to Vol. 2. *Health criteria and other supporting information* (Geneva 1998).

5. Directive 2004/107/EC of the European Parliament and of the Council of 15 December 2004 relating to arsenic, cadmium, mercury, nickel and polycyclic aromatic hydrocarbons in ambient air, OJ L 23 (2005), p. 3.

6. F. Kafilzadeh, A.H.Shiva, R.Malekpour, "Determination of Polycilyc Aromatic Hydrocarbons in Water and Sediments of Kor River, Iran", Middle-East Journal of Scientific Research 10, 1–7 (2011).

7. A. Soceanu, S. D. Stanciu, V. Popescu, "Polycyclic Aromatic Hydrocarbons in vegetables grown in urban and rural areas", Environmental Engineering and Management Journal, Vol. 13, No. 9., 2311-2315 (2014).

8. B. Maliszewska-Kordybach, "Sources, Concentrations, Fate and Effects of Polycyclic Aromatic Hydrocarbons (PAHs) in the Environment", Polish Journal of Environmental Studies, Vol. 8, No. 3, 131–136 (1999).

9. M. Larsson, "Integrated Bioassay- and Chemical Analysis in Risk Assessment of Remediated PAH-Contaminated Soils", Licentiate Thesis, Öbero University, (2009).

10. T. Wenzl, R. Simon, J. Kleiner, E. Anklam, "Analytical methods for polycyclic aromatic hydrocarbons (PAHs) in food and the environment needed for new food legislation in the European Union", Trends in Analytical Chemistry, Vol. 25, No. 7, 716–725 (2006).

11. T. Sakuma et al., "Analysis of Polycyclic Aromatic Hydrocarbons (PAH), Alkylated Derivatives, and Photo-degradation Products in Environmenta and Food Samples using LC-FLD-MS/MS with Q TRAP Technology", AB Sciex Food & Environmental brochure, p. 1-7, (2011).

12. T. C. O'Haver, "Derivative and Wavelength Modulation Spectrometry", Analytical Chemistry vol. 51 No. 1, 91-100 (1979).

13. F. H. Lisseberger, W. L. Wilcock, “Properties of All-Dielectric Interference Filters. II. Filters in Parallel Beams of Light Incident Obliquely and in Convergent Beams”, Journal of the Optical Society of America, Vol. 49, No. 2, 126-130 (1989).
14. G. B. Rieker, J. B. Jeffries, R. K. Hanson, “Calibration-free wavelength-modulation spectroscopy for measurements of gas temperature and concentration in harsh environments”, Applied Optics, Vol. 48, No. 29, 5546–5560 (2009).

Lihtlitsents lõputöö reprodutseerimiseks ja lõputöö üldsusele kättesaadavaks tegemiseks

Mina, Dmitri Lanevski,

1. annan Tartu Ülikoolile tasuta loa (lihtlitsentsi) enda loodud teose

INTERFERENCE FILTER TILTING FOR DETECTION OF POLYCYCLIC AROMATIC HYDROCARBONS AT THE SECOND HARMONIC OF WAVELENGTH MODULATION FREQUENCY

mille juhendajad on Koit Mauring ja Eric Tkczyk,

1.1. reprodutseerimiseks säilitamise ja üldsusele kättesaadavaks tegemise eesmärgil, sealhulgas digitaalarhiivi DSpace-is lisamise eesmärgil kuni autoriõiguse kehtivuse tähtaja lõppemiseni;
1.2. üldsusele kättesaadavaks tegemiseks Tartu Ülikooli veebikeskkonna kaudu, sealhulgas digitaalarhiivi DSpace´i kaudu kuni autoriõiguse kehtivuse tähtaja lõppemiseni.

2. olen teadlik, et punktis 1 nimetatud õigused jäävad alles ka autorile.

3. kinnitan, et lihtlitsentsi andmisega ei rikuta teiste isikute intellektuaalomandi ega isikuandmete kaitse seadusest tulenevaid õigusi.

Tartus/Tallinnas/Narvas/Pärnus/Viljandis, **30.05.2016**